Theory of Polymer Adsorption and Colloid Stabilization in Supercritical Fluids. 1. Homopolymer Stabilizers

J. Carson Meredith and Keith P. Johnston*

Department of Chemical Engineering University of Texas at Austin, Austin, Texas 78712

Received February 19, 1998; Revised Manuscript Received May 26, 1998

ABSTRACT: Homopolymer adsorption and stabilization of colloids in compressible supercritical solvents are modeled with the lattice-fluid self-consistent field theory (LFSCF). Adsorption at a single surface is characterized versus bulk solvent density for various polymer chain lengths, solubilities, and concentrations. As solvent density is lowered, adsorbed chains first collapse due to the loss in solvent quality, and then expand due to an increase in adsorption that raises the excluded volume. This collapse-to-expansion transition in layer thickness occurs just above the critical solution density for a bulk polymer solution. Colloid stability is examined by calculating the free energy of interaction of two parallel surfaces coated with adsorbed polymer. Above a threshold concentration and molecular weight, the surfaces are stabilized at high density. As density is lowered, the entropically favorable expansion of solvent from the interface causes flocculation at the critical solution density of the homopolymer in bulk solution, in agreement with recent light scattering experiments. At lower concentrations, bridging occurs and stabilization is not possible, even in a high density, good solvent.

Introduction

The potential and current applications of microemulsions, emulsions, and latexes in supercritical fluids such as CO_2 abound, as reviewed recently.[1−3] Emulsions and latexes may be stabilized with block copolymers or homopolymers to prevent flocculation. Of critical importance is the balance of interactions between the dispersed phase, stabilizer, and the solvent. Because CO_2 has a very low polarizability and no dipole moment, most polymers and surfactants are not solvated well enough to stabilize colloids in CO_2. The ability to design steric stabilizers for the interface between organics, polymers, or solids and CO_2, offers exciting new opportunities in chemical manufacturing including polymerizations,[4−9] formation of micron and submicron polymer particles in spray processes,[10,11] extractions, including heavy metals,[3,12,13] and replacement of chlorofluorocarbons and other solvents in cleaning and purification processes.[3] What is needed at this stage in stabilizer design is a fundamental understanding of how polymer structure affects adsorption and stabilization in dispersions and emulsions.

In a compressible solvent, as temperature is raised at constant pressure, solvent quality decreases, and polymer chains collapse as the lower critical solution temperature (LCST) phase boundary is approached. The loss in solvent quality is due primarily to a decrease in solvent density.[14] The same phase boundary is approached as density (pressure) is lowered at constant temperature. In this case, the critical point is an upper critical solution density (UCSD). The system gains entropy when the solvent expands away from the polymer chain into the lower density bulk solution. With less solvent present to screen attractive intrachain interactions, the chains collapse and ultimately phase separation occurs. Whereas collapse near an upper critical solution temperature (UCST) phase boundary is energetically driven, collapse near the LCST phase boundary is entropically driven.[15,16] Just as the UCST and LCST become Θ temperatures at infinite molecular weight, there is a Θ density that corresponds to the UCSD.

Emulsion droplets or dispersed phase particles may be stabilized by adsorbed polymers due to the unfavorable entropy loss when the polymer chains overlap during a collision. The phase behavior of the polymeric stabilizer in bulk solvent is a key indicator of the conditions where stabilization of a dispersed phase is possible. Figure 1 demonstrates an analogy between polymers on surfaces and polymers in bulk for a compressible solvent. In both cases at high solvent density, the polymer is in a good solvent where it adopts expanded conformations. At low solvent density, the polymer collapses as solvent expands away from the chains to raise the entropy. For this reason, in bulk solution a polymer-enriched phase separates from the solvent-rich phase at low densities. For chains on surfaces, solvent expansion at low densities creates an attractive force between the layers of adsorbed polymer and the surfaces flocculate, forming polymer-enriched domains between them.

Napper has discussed the correlation between the Θ point of polymeric stabilizer in bulk solution and the critical flocculation point of a sterically stabilized colloid in subcritical fluids.[17] If the molecular weight and adsorbed amount are above certain thresholds, the critical flocculation temperature (CFT) of a colloid occurs near the Θ temperature for the stabilizer in bulk solution. This relationship is particularly true for grafted and block copolymer stabilizers, which tend to adsorb strongly. A unique aspect of dispersions in supercritical fluids is the large density dependence of fluid properties, which influences polymer phase behavior and colloid stability. In this sense, supercritical fluids offer a unique vantage point for understanding the effect of solvent quality on the structure of polymers adsorbed at interfaces. As solvent density is decreased at constant temperature, the dispersion becomes unstable at a critical flocculation density (CFD).[18−20]

Recent experiments have examined solvent density effects on latex and emulsion stability in compressible

S0024-9297(98)00259-9 CCC: $15.00
Published on Web 07/24/1998

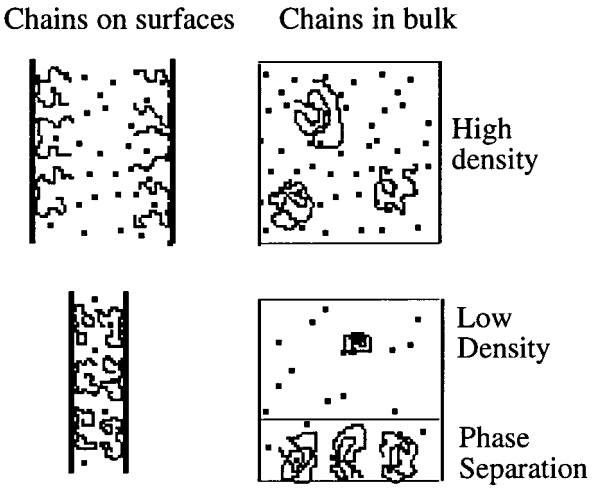

Figure 1. Schematic representation of analogy between bulk polymer solution phase behavior and flocculation of polymer-coated surfaces.

media. Polymers with low surface tensions and thus low cohesive energy densities tend to be the most soluble in CO_2.[21] The stabilization of poly(2-ethyl hexyl acrylate) (PEHA) emulsions in liquid and supercritical CO_2 was recently studied with both dynamic light scattering[20] and turbidimetry.[19] The homopolymer poly(1,1-dihydroperfluorooctyl acrylate) (PFOA), is highly soluble in CO_2 and is a very effective stabilizer for these emulsions and for dispersion polymerization.[4−9] The CFD is the same as the critical solution density (CSD) of PFOA in bulk solvent. PFOA also enhances the stability of PMMA dispersions produced by precipitation in a compressed fluid antisolvent.[22]

A variety of theoretical approaches have been utilized to treat stabilization by adsorbed polymer in incompressible solvents. The lattice self-consistent field (SCF) theory of Scheutjens and Fleer[23] has been applied to both homopolymer[24] and copolymer stabilizers.[25,26] The SCF theories give detailed information about equilibrium interfacial properties as a function of chain−chain and chain−solvent interactions, adsorption energy, and polymer structure. Off lattice analytical[27] and numerical[28] SCF approaches have examined the effect of solvent quality on grafted and adsorbed polymer layers. Many of the advantages and anomalies of supercritical fluid colloids are due to the free volume and high compressibility of the solvent. By introducing holes into the lattice, the SCF theory of Scheutjens and Fleer was extended to model *end-grafted* polymers in compressible solvents[18] and is termed the lattice-fluid self-consistent field theory (LFSCF).

Our objective is to utilize the LFSCF theory to model adsorption of homopolymers at a planar surface and free energies of interaction between such surfaces. Copolymers will be considered in part 2.[29] We wish to understand how solvent density affects adsorbed amount and layer thickness, which in turn influences colloid stability. Results are presented for the adsorbed amount, fraction of adsorbed segments, and adsorbed layer thickness and are compared with relevant experiments. The effects of polymer properties such as solubility, adsorption energy, molecular weight, and concentration are explored. The effect of solvent density on the collapse of the adsorbed polymers is compared with the UCSD for the polymer in bulk solution. When the polymer concentration is sufficiently high, colloid stability decreases with decreasing bulk solvent density. The CFD is determined from the interaction free energy between two homopolymer-coated surfaces and compared with the critical solution density (CSD) of the stabilizer in bulk solution. The LFSCF results are compared with the aforementioned stability experiments that used PFOA-based stabilizers in supercritical CO_2. The interaction free energy is explained in terms of the corresponding enthalpy and entropy changes. A distinction is made for high and low concentrations of polymer. At low concentration, we expect bridging of homopolymer between two surfaces to induce flocculation.

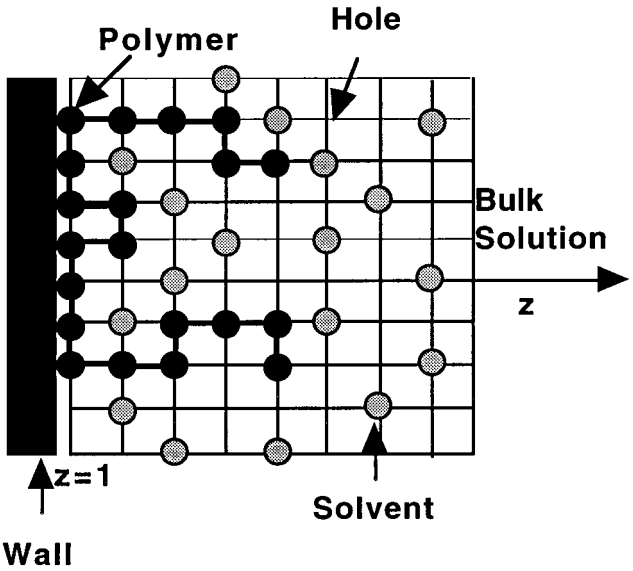

Figure 2. Two-dimensional representation of the adsorbent surface and lattice occupied with polymer, solvent, and hole segments.

Theory

Lattice-Fluid Self-Consistent Field Theory. The LFSCF theory of Peck[18] is extended here to model adsorption of homopolymers onto a solid, impermeable surface, as shown in Figure 2. The lattice layers numbered $z = 1, 2, ..., M$ each have L lattice sites for a total of ML lattice sites. Each site is occupied by a solvent (s), a chain (c) segment, or a hole (o). Polymer molecules are represented as chains of length r_c. The reader is referred to previous publications[18,30] and the *Appendix* for further details of the derivation.

The main goal of SCF theory is to find the equilibrium distribution of all molecules over all possible chain conformations on the lattice. As a simplifying assumption, lateral density fluctuations within each layer are neglected. As a consequence, only the distance in the z direction is relevant in the calculation of interaction energies and interfacial properties. A segment feels a mean potential due to neighboring segments in the same and adjacent layers. This mean field assumption is common to all forms of the SCF theory. In addition, the self-excluded volume of a chain is neglected, although *intersegmental* excluded volume interactions are included. The equilibrium distribution of polymer and solvent segments is found by using Lagrange multipliers to maximize the grand canonical partition function, $\Xi(\mu,V,T)$. At the beginning of each LFSCF calculation the temperature, pressure, and polymer bulk concentration, ϕ^b, are specified. As in the lattice-fluid theory, ϕ^b is a

segment fraction. The final result is the equilibrium set of segment concentrations in each layer, $\{f_i(z)\}$. From this equilibrium configuration all relevant properties are calculated. Because fluctuations are neglected, the LFSCF theory will not model the long-range density fluctuations that occur near the solvent critical point. Thus, this study does not consider conditions too close to the critical point. (The temperature is $1.05T_c$, but the lowest density considered is $\sim 1.4\rho_c$).

In this paper, chain adsorption is characterized by the number of adsorbed chains per unit lattice area, $\sigma = \Gamma/r_c$. The parameter Γ is the absolute amount of adsorbed chain segments per unit area and is given by

$$\Gamma = \sum_z (f_c(z) - f_{c,\text{free}}(z)) \tag{1}$$

where $f_c(z)$ is the total fraction of chain segments c (per unit area) in layer z and $f_{c,\text{free}}(z)$ is the fraction of nonadsorbing chain segments in layer z. This absolute adsorbed amount in a given layer approaches zero as z increases away from the surface and concentrations approach their bulk solution values. A chain is counted as adsorbed when at least one segment is adjacent to a surface. The parameter σ is reduced according to $\sigma^* = \sigma\pi(R_g)^2$ where R_g is the bulk radius of gyration. For $\sigma^* \ll 1$, the chains are isolated from one another on the surface, and when $\sigma^* > 1$, the chains begin to overlap. Due to the neglect of fluctuations and the chain self-excluded volume, SCF theory is most applicable to the case where chains are overlapping ($\sigma^* > 1$) on the surface. When chains overlap, each chain is shielded from interacting with itself, and the self-excluded volume is negligible. When $\sigma^* \ll 1$, results from LFSCF are expected to be only qualitatively correct. The limitations of SCF theory have been discussed in light of exact results from lattice Monte Carlo simulations for incompressible fluids.[31,32]

We calculate the layer thickness as the root-mean-square surface-to-chain-end distance, which is given by

$$h = \left(\sum_z z^2 (G_c(z,r_c|1) - G_{c,\text{free}}(z,r_c|1))\right)^{1/2} \tag{2}$$

where $G_c(z,r_c|1)$ is the normalized probability of finding a chain-end segment in layer z.[18]

Interaction Free Energies. The interaction free energy between two polymer coated surfaces is given by $\Delta G_{\text{total}} = \Delta G_{\text{scf}} + \Delta G_{\text{Ham}}$. The parameter ΔG_{scf} is the free energy obtained using LFSCF theory and results from intra- and intersegment interactions of solvent and polymer. The parameter ΔG_{scf} is calculated according to the restricted equilibrium assumption,[24] where the collision of two surfaces is modeled on a time scale shorter than the time required for a polymer chain to desorb and diffuse out of the interface. As the surfaces are brought together at constant temperature, T, and pressure, P, the solvent may freely equilibrate between the bulk and interfacial region, but the adsorbed chains cannot leave the interfacial region. The adsorbed chains can equilibrate *within* the interfacial region between the surfaces.

The Hamaker contribution, G_{Ham}, is due to the van der Waals interaction between the surfaces themselves, excluding the homopolymer chains. For infinitely thick flat plates, the Hamaker energy is given by $-A/12\pi z^2$ where z is the separation distance. In calculating ΔG_{Ham}, we take into account the retardation of van der Waals energies, which becomes important at distances greater than $\sim$150 Å or 35 lattice layers.[33]

Selection of Parameters. In the lattice-fluid theory,[16,34] each molecule of type i is described by three parameters: r_i the number of i segments per molecule; P_i^* the segmental cohesive energy density of the random close packed reference fluid; and v_i^*, the volume per segment. The magnitude of P_i^* determines the strength of pure component interactions, whereas the difference in $(P_i^*)^{1/2}$ values determines the strength of intermolecular interactions (e.g., $\chi_{ij} = (P_i^{*1/2} - P_j^{*1/2})^2 v^*/kT$). The solvent parameters were chosen by a least-squares fit to the density versus pressure isotherm for CO_2 at $T = 45$ °C ($T_r = 1.05$). These parameters are $r_s = 1$, $P_s^* = 1000$ atm, and $v^* = 52$ cm^3/mol. For simplicity, the segmental volume for the polymer segments was set equal to that of the solvent. The reduced density, $\tilde{\rho}$, is defined as ρ/ρ^*, where ρ is the actual density and ρ^* is the characteristic density of a random close-packed reference fluid and is related to the other lattice fluid parameters by $\rho^* = rM_w/v^*$.[16] The reduced density $\tilde{\rho}$ is also the volume occupied by chain and solvent segments divided by the total volume including holes. Hence $\tilde{\rho} = 1$ in the high-density, incompressible limit. Comparison with experimental densities and temperatures is best done by using units reduced with respect to the critical properties. The critical properties of the model solvent are $\tilde{\rho}_c = 0.5$ and $T_c = 319$ K.

Parameters for the model homopolymers were chosen relative to those of the solvent to represent the various types of polymers studied in experiments. For example, P_c^* for the homopolymer should be relatively close to P_s^* in an attempt to model a polymer that is quite soluble in CO_2, such PFOA. A high solubility in CO_2 requires a low pure polymer surface free energy,[21] γ, a property closely related to the cohesive energy density. Because CO_2 has a very low cohesive energy density, the most soluble polymers (e.g., PFOA) have the lowest γ values, and hence have low P_c^* values. Because $P_s^* = 1000$ atm, P_c^* values of 1000, 1200, and 1400 atm were used to model polymers with cohesive energy densities near (e.g., PFOA) and somewhat above (e.g., poly(dimethylsiloxane)) that of the solvent.

In addition to the three lattice fluid parameters, the adsorption energy of a polymer segment relative to the solvent, ϵ_{AW}, must be specified. As described in the *Appendix*, ϵ_{AW} is equivalent to χ_s that is used often in other SCF theories.[30] Values between 0.5 and 5 kT are reported by van der Beek et al.[30,35] for several common polymers including polystyrene (PS) and poly(ethylene oxide) (PEO) on silica and alumina. Because of the nature of homopolymer adsorption, if ϵ_{AW} is too large, the homopolymer adopts a flat layer incapable of stabilization. If ϵ_{AW} is too low, there will be insufficient adsorption. The critical adsorption energy, below which the chain does not adsorb, was found to be 0.284 for the $r_c = 1000$, $P_c^* = 1200$ chain. (Scheutjens and Fleer obtained $\epsilon_{AW} = 0.288$ for a similar model.[36]) It is known that although PFOA adsorbs weakly to a PEHA interface, it does adsorb strongly enough to stabilize a PEHA-in-CO_2 emulsion.[19] We therefore chose $\epsilon_{AW} = 0.5\ kT$ for most of the calculations in this paper, because it is above the critical adsorption energy but below 1 kT. The adsorption of PS onto silica from liquid solvents has been modeled successfully with a similar value, $\epsilon_{AW} = 0.42$. We have also examined higher and lower values

Table 1. Lattice-Fluid Parameters and Chain Properties

segment type	r	P^* (atm)	ϵ_{AW} (kT)	R_g
solvent (S)	1	1000	0	
homopolymer (A)	300	1200	0.5, 1.0	13.0
	1000	1200	0.25, 0.3, 0.5	26.2
	3000	1000	0.5	50.4
	3000	1200	0.5	50.1
	3000	1400	0.5	49.2

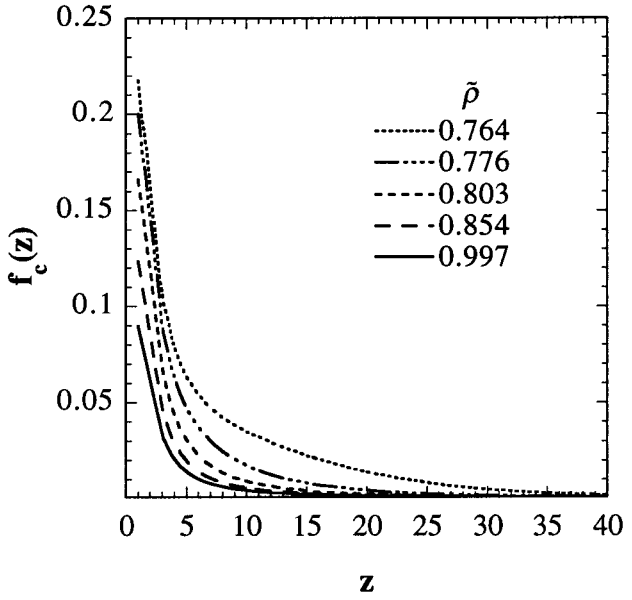

Figure 3. Adsorbed segment volume fraction profiles at several densities for $r_c = 1000$ (chain length), $\epsilon_{AW} = 0.5\ kT$ (adsorption energy), $P_c^* = 1200$ atm (cohesive energy density), and $\phi^b = 10^{-3}$ (concentration).

of ϵ_{AW}, as indicated in Table 1. Our high adsorption energies and low concentrations eliminate the need to consider depletion forces induced by nonadsorbing polymer, because there is always a surface excess.

The Hamaker coefficient for the surfaces was taken as that of PS, $A_{PS} = 16\ kT$.[37] The coefficient A_{PS} must be modified to account for the solvent, CO_2, with $A_{PS,CO_2} = (A_{PS} + A_{CO_2} - (A_{PS}A_{CO_2})^{1/2})$.[37] The solvent Hamaker constant is found using $A_{CO_2} = 4\pi^2(\rho N_A/M_w)^2\epsilon_{CO_2}(\sigma_{CO_2})^6 = 22.5\bar{\rho}^2\ kT$, where N_A is Avogadros number and M_w is the molecular weight. The Leonard-Jones (LJ) parameters used for CO_2 were $\epsilon_{CO_2} = 192.25k$ (K) and $\sigma_{CO_2} = 4.416$ Å.[38]

Results and Discussion

Adsorbed Amounts, Surface Coverage, and Layer Thickness. Figure 3 shows concentration profiles of adsorbed homopolymer at various densities. All other equilibrium properties are calculated from the concentration profile. Half or more of the total chain density is confined to the first few layers, and the remaining chain density tapers off over a large distance. Much of each chain is close to the surface in adsorbed trains and short loops, with tails dangling into the solvent. For comparison, the bulk radius-of-gyration of the homopolymer is 26 lattice units at $\tilde{\rho} = 1$. As density is decreased from the incompressible limit ($\tilde{\rho} = 0.997$) the amount adsorbed increases, causing greater extension of the tails, but the shape of the profile does not change significantly.

Figure 4a gives the reduced amount adsorbed, σ^*, as a function of reduced solvent density for homopolymers with lengths 1000 and 3000 at several concentrations.

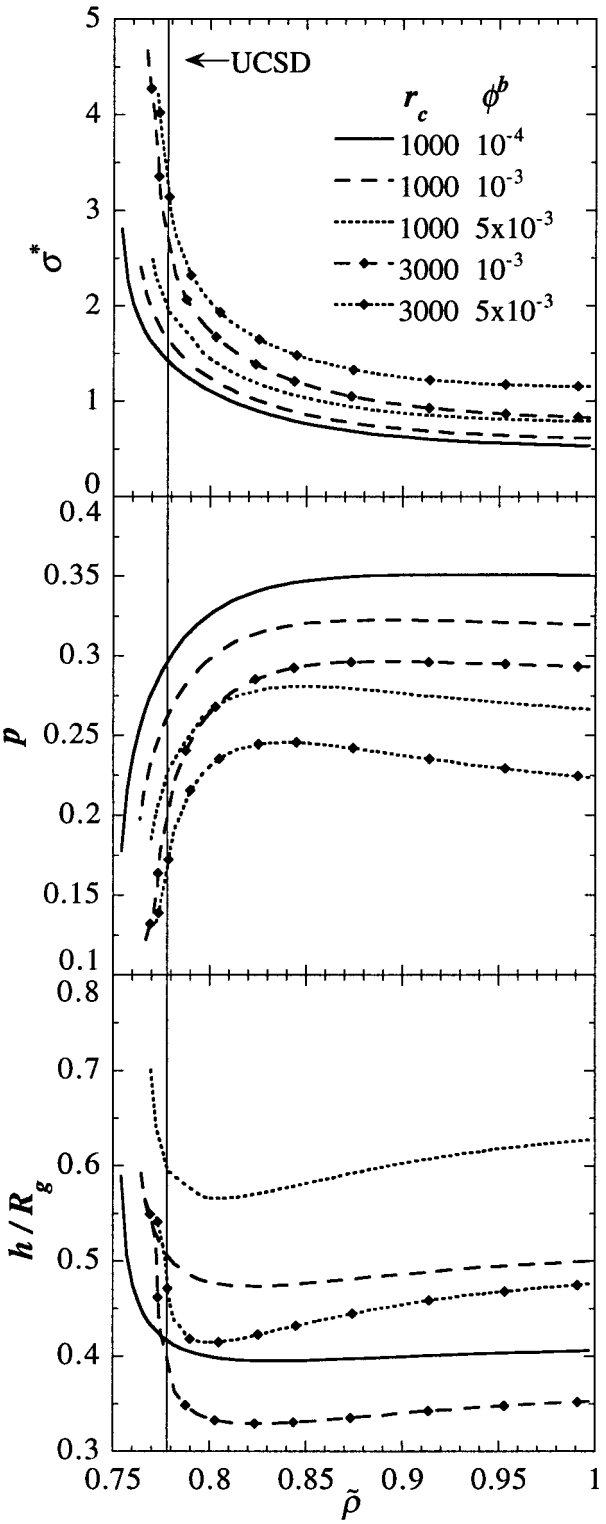

Figure 4. (a) Adsorbed amount (σ^*), (b) bound fraction (p), and (c) layer thickness (h/R_g (good solvent)) versus reduced bulk solution density, $\tilde{\rho}$, for homopolymers at a single surface. Adsorption energy, ϵ_{AW}, is 0.5 kT, and cohesive energy density, $P_c^* = 1200$ atm. Chain length and concentration are indicated in the legend. All other parameters are in Table 1. Arrows indicate the upper critical solution density (UCSD) in bulk solution.

At high $\tilde{\rho}$, in the good solvent regime, σ^* is <1 for $r_c = 1000$, and the chains do not overlap significantly with their neighbors on the surface. For $r_c = 3000$, $\sigma^* > 1$ at all densities. As $\tilde{\rho}$ decreases, the bulk fluid becomes a poorer solvent and more chains adsorb. When $\sigma^* \approx 1$,

the adsorbed chains begin to overlap. As solvent density is lowered beyond this point, σ^* values begin to increase more rapidly and the area occupied by an adsorbed chain ($1/\sigma^*$) decreases. Thus, as $\tilde{\rho}$ is decreased, both the number of adsorbed chains and the degree of overlap increases.

The effect of solvent quality on adsorbed amount is well known in liquid solvents near the UCST. For example, the adsorbed amount of PS from cyclohexane onto chrome increases as temperature is decreased toward the bulk UCST.[39] In our case, solvent quality is decreased by lowering solvent density, approaching the bulk UCSD, which is analogous to the LCST. For comparison, the UCSDs for the $r_c = 1000$ and 3000 chains, determined from the lattice fluid theory stability condition,[16] are marked by vertical lines in Figure 4. The UCSD for $r_c = \infty$ is the Θ density ($\tilde{\rho}_\theta$). For the long chains in this paper ($r_c = 1000$ and 3000), the UCSD at finite molecular weight and $\tilde{\rho}_\theta$ are virtually indistinguishable. The σ^* values increase rapidly in the region near the UCSD for the polymer in bulk solution. At the UCSD, the surface becomes a nucleation point for phase separation by adsorption. Although we decrease solvent density to values just below the UCSD, the LFSCF theory does not account for formation of a homopolymer-rich condensed phase, which would reduce free polymer in solution available for adsorption. However, this is only an issue close to the critical concentration of $\phi^b \approx 0.015$, which is higher than the ϕ^b values considered here.[29]

The magnitude of σ^* increases with both the degree of polymerization and bulk concentration, as is also observed experimentally in conventional liquid solvents.[39,40] Increasing r_c reduces the solubility in bulk solution at a given solvent density, and as a result more polymer migrates to the surface. Adsorbed amount increases only moderately with concentration, indicating the system is in the plateau region on the adsorption isotherm, which is described by Scheutjens and Fleer for a homopolymer with similar properties in an incompressible solvent.[23]

In Figure 4b, as $\tilde{\rho}$ is decreased starting from unity, the average fraction of segments bound to the surface (p) increases slightly. However, near the UCSD, p decreases sharply, as solvent strength diminishes, and fewer anchoring sites are required to hold a chain at the surface. The decrease in p is related directly to the increase in adsorption and the resulting overlap transition seen in Figure 4a. With less room on the surface for anchoring sites, a larger fraction of the chain may exist in either tails or loops. It is well established from previous SCF studies of homopolymer adsorption with similar parameters that most of the unbound segments exist as free tails, with relatively few segments in loops.[36] As r_c and ϕ^b are increased, adsorbed amount increases, the surface becomes more crowded, and the bound fraction decreases. The following picture of a structural transition near the UCSD emerges: as solvent density is decreased, more chains adsorb, thereby increasing the surface coverage, and the previously adsorbed chains begin to release some adsorbed segments from the surface. With longer tails, more adsorbed chains, and less space available on the surface, overlap increases significantly (entropically unfavorable), but this penalty is balanced by the decrease in bulk solvent quality and the energy gained by adsorbing segments.

Table 2. Fraction of Bound Segments (p) from Experiment and LFSCF Theory

source	ϵ_{AW} (kT)	$M_w \times 10^{-3}$	ϕ^b	p
experiment[a]	0.42	42.8	0.0017	0.32
	0.42	102	0.0016	0.26
	0.42	775	0.0016	0.24
LFSCF theory[b]	0.5	50	0.001	0.32
	0.3	50	0.001	0.035
	0.25	50	0.001	0.01

[a] PS/trichloroethylene (good solvent)/silica at 25 °C (ref 39). [b] $r_c = 1000$, $P_c^* = 1200$ at $\tilde{\rho} = 0.85$ (good solvent), and $T/T_c = 1.05$, we assign an arbitrary segmental molecular weight of 50.

Bound fractions have been measured spectroscopically for homopolymer adsorption at surfaces in liquid solvents.[41,42] Table 2 shows data for PS adsorption to silica from trichloroethylene (a good solvent). Using the Scheutjens and Fleer SCF theory, Kawaguchi et al.[39] obtained an adsorption energy of 0.42 kT, which is close to the 0.5 kT used in our study. At a molecular weight of 42 800 and concentration of 0.17 wt %, the bound fraction was 0.32, which is in excellent agreement with our value of $p = 0.32$ at $r_c = 1000$ ($M_w \approx 50\,000$), $\phi^b = 10^{-3}$ (0.1 wt %), and $\tilde{\rho} = 0.85$. The agreement results primarily from the high liquidlike solvent density (good solvent regime) used in this LFSCF calculation. The data in Table 2 verify experimentally the decrease of p with molecular weight seen in Figure 4b. Takahashi[42] gives experimental evidence for the decrease in p with increased adsorption for PS on silica, which is qualitatively similar to what we observe in Figure 3b for a factor of 2 to 3 increase in adsorption. For liquid solvents, the amount adsorbed can be increased by increasing bulk concentration or decreasing temperature. Although the methods used to increase adsorption (e.g., temperature or density) are different in liquid and supercritical solvents, the effect of adsorbed amount on structure is somewhat similar.

Table 2 also shows that lowering ϵ_{AW} from 0.5 to 0.3 to 0.25 causes a rapid decrease in the bound fraction. The σ^* values fall dramatically as well, passing from adsorption to depletion at $\epsilon_{AW} = 0.284$, which is thus the critical adsorption energy for the $r_c = 1000$ chains. Also, at $\epsilon_{AW} = 1.0$ (not shown), the chains begin to adopt flatter conformations at the surface, with bound fractions approaching 0.6. With so few segments in tails at $\epsilon_{AW} = 1.0$, significant steric stabilization is not expected.

Figure 4c shows h/R_g, the r.m.s. surface-to-chain-end distance divided by the bulk radius-of-gyration in a good solvent (high-density limit). The parameter R_g is found from Flory's lattice theory[43] and is given in Table 1. Figure 4c indicates that most h values are only ~40−70% of R_g. Scaling theory[40] predicts that in good solvent the adsorbed homopolymer layer thickness scales as $r_c^{2/5}$ compared with $r_c^{3/5}$ for R_g in bulk solution. Thus, the adsorbed homopolymer layer adopts a conformation that is compact relative to bulk dimensions because each segment is attracted to the surface. This result is in contrast to strongly adsorbed diblock copolymers, which are often expanded relative to bulk dimensions, due to the excluded volume of the nonadsorbing blocks.[29]

As solvent density is lowered, h/R_g indicates that tails collapse due to the loss in solvent quality. The amount of collapse is small at $r_c = 1000$ and low concentrations, but more collapse is observed as r_c and ϕ^b increase. Longer tails are more susceptible to incompatibility with a solvent as is evident in the lattice-fluid expression for

Table 3. Minima in Layer Thickness and Critical Flocculation Density Compared with Θ Density and UCSD in Bulk Solution

r_c	ϕ^b	P_c^*	$\tilde{\rho}$	UCSD	$\tilde{\rho}(h_{min})$	CFD
300	10^{-4}	1200	0.784	0.769	0.811	flocc
1000	10^{-4}	1200	0.784	0.778	0.837	flocc
1000	10^{-3}	1200	0.784	0.778	0.823	flocc
1000	2.5×10^{-3}	1200	0.784	0.778	0.813	0.79
1000	5×10^{-3}	1200	0.784	0.778	0.805	0.77
3000	10^{-3}	1000	0.736	0.733	0.776	flocc
3000	10^{-3}	1200	0.784	0.780	0.824	flocc
3000	2.5×10^{-3}	1200	0.784	0.780	0.809	0.775
3000	10^{-3}	1400	0.829	0.825	0.865	0.865

the chemical potential.[16] As solvent density is lowered below the UCSD, h/R_g shows a dramatic increase, due to the increased adsorption and overlap (Figure 4a). Here the bound fractions begin to decrease (Figure 4b) creating longer tails, and the longer, overlapping tails exclude volume from one another and create a thicker layer (Figure 4c). Thus, there are two competing factors which influence h as $\tilde{\rho}$ is decreased: (1) the tails of adsorbed chains collapse, decreasing h, and (2) chains add to the surface, increasing h. Starting from a good solvent and lowering solvent density, collapse wins the battle at first. A minimum in h occurs where the effects of these mechanisms are balanced, and at lower densities a growth of the layer is observed due to overlap. The balance of layer collapse and expansion is related to the approach to the critical point of the homopolymer in bulk solution as solvent density is lowered. Table 3 compares the $\tilde{\rho}(h_{min})$ where the minimum thickness occurs to the UCSD for various values of r_c, ϕ^b, and P_c^*. The parameter $\tilde{\rho}(h_{min})$ is consistently greater than the UCSD, but approaches the UCSD as r_c and ϕ^b increase.

Experiments confirm that adsorbed layers of PS in cyclohexane collapse as temperature is decreased toward the bulk Θ temperature.[39] A more recent experiment on adsorbed PS in cyclopentane reveals an expansion of layer thickness from $h/R_g = 0.34$ to 0.56 as temperature is decreased below T_θ.[44] Poly(*N*-isopropylacrylamide) adsorbed on PS in water shows a collapse-to-expansion transition as temperature is raised through the LCST of the polymer in bulk solution.[45] These results show that both collapse and expansion mechanisms are operative as solvent quality is reduced in liquid as well as supercritical solvents.

Consider the adsorption energy. For the chain lengths and concentrations of Figure 4, the layer thickness actually decreases when ϵ_{AW} is increased from 0.5 to 1.0 kT (not shown). The flattened conformation allows more segments on each chain to interact with the surface. An adsorption energy of 0.5 kT strikes a balance between the extremes of low adsorbed amount and high adsorbed amount with thin layers.

Another important polymer property is the chain cohesive energy density (CED), which governs the magnitude of solvent−chain and chain−chain dispersion interactions. In the LFSCF theory, the CED is equal to $\tilde{\rho}^2 P_c^*$. At $P_c^* = 1000$, the P_c^* of the polymer is equal to that of the solvent. As P_c^* increases at constant density the polymer becomes progressively less soluble. Hence, as P_c^* increases, the bulk coexistence curve for the polymer−solvent mixture shifts to higher values of pressure and density. For this reason, the shapes and magnitudes of the three curves for σ^*, p, and h/R_g in Figure 5a are similar but shift to higher density as P_c^* increases. The h/R_g values shift with $\tilde{\rho}$ to about the same extent as the UCSDs (vertical lines in Figure 5).

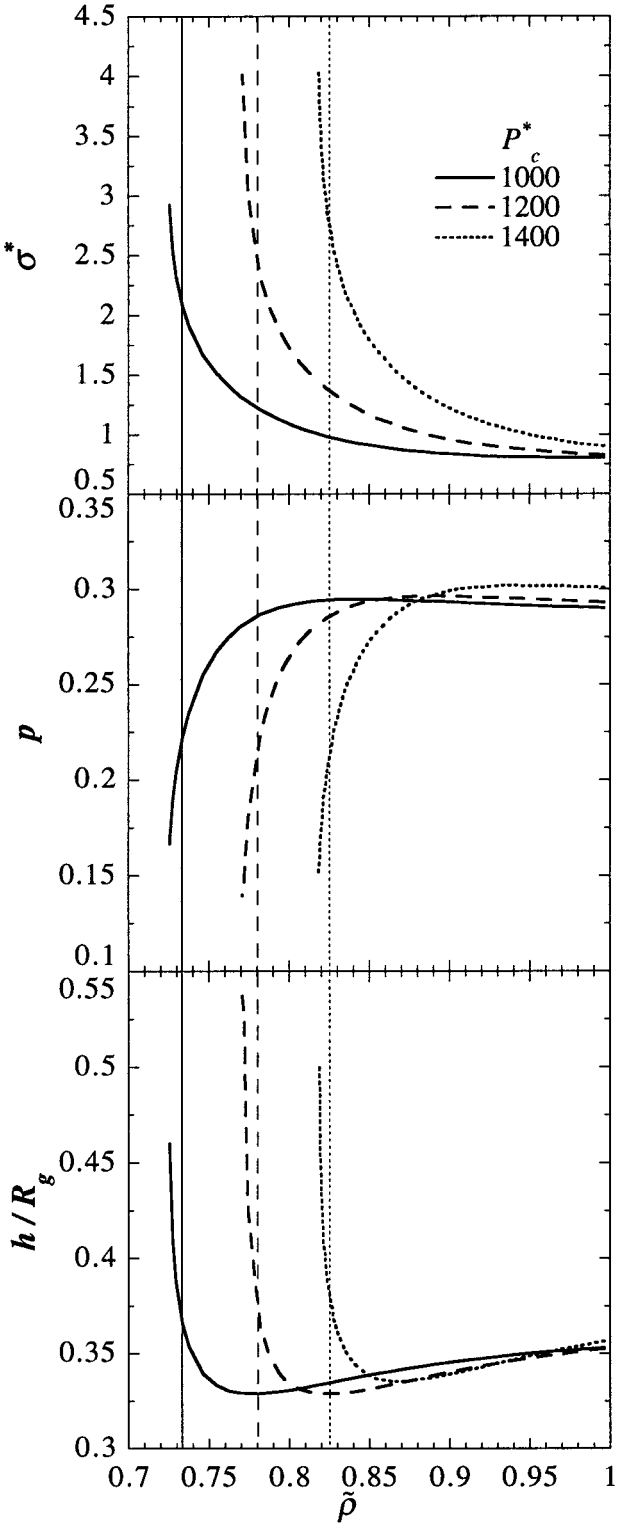

Figure 5. (a) σ^*, (b) p, and (c) h/R_g (good solvent) versus reduced bulk solution density, $\tilde{\rho}$, for $P_c^* = 1000$, 1200, and 1400 atm (cohesive energy density); $r_c = 3000$ and $\epsilon_{AW} = 0.5$ kT (adsorption energy). Vertical lines indicate the UCSD in bulk solution at each P_c^*.

Unlike the case for P_c^*, changes in other chain properties, such as r_c, ϵ_{AW}, or ϕ^b, shift the actual magnitude of the amount adsorbed, the bound fraction, and the layer thickness without significantly changing the transition density (Figure 4). Thus r_c, ϵ_{AW}, and ϕ^b can be adjusted to set a desired layer thickness, adsorbed

amount, and degree of overlap to influence steric stabilization. The chain CED only shifts the solvent density at which important structural changes occur, and hence should not affect whether steric stabilization is possible, if the density is sufficiently large.

In our LFSCF calculations, the CED of the chain was varied at *constant* adsorption energy. In a real homopolymer−solvent−surface system a change in the chemical structure of the chain will modify the CED and chain−surface interactions simultaneously. The inseparability of CED and adsorption energy contributes to the difficulty in finding a homopolymer stabilizer for supercritical CO_2. Such a stabilizer must have a low CED to ensure solubility and extension of the tails in CO_2 at reasonable pressures, but if the CED is too low, ϵ_{AW} may be too small for adsorption to typical surfaces.

Free Energy of Interaction. Figure 6a shows ΔG_{scf}, the free energy due solely to the interactions between two adsorbed polymer layers and the solvent at $\phi^b = 2.5 \times 10^{-3}$. The free energy is repulsive at high densities, and an attractive minimum appears below $\tilde{\rho} = 0.777$. ΔG_{Ham}, which is due solely to Hamaker forces of attraction between the surfaces in the solvent (without including homopolymer), is given in Figure 6b. The total interaction, $\Delta G_{scf} + \Delta G_{Ham}$, indicates a repulsive barrier against flocculation at densities above 0.78 (Figure 6c), which is close to the UCSD of 0.778. Below the UCSD, the shape of the free energy in Figure 6c changes and attractive minima appear, arising from both Hamaker and LCST-type attraction. Flocculation will occur when the minimum is deeper than the average thermal energy of colloidal particles, $3/2kT$. Using an estimated contact area of 10^4 lattice units for 500 nm particles, the flocculation threshold is on the order of $\Delta G_{floc}/LkT \approx 10^{-4}$.[29] Thus, Figure 6c indicates that flocculation will occur near the UCSD of the polymer in bulk solution. The flocculation threshold free energy is only an order of magnitude estimate based on the kinetic energy of colloidal particles. The concentration dependence of the flocculation threshold free energy has been neglected. Thus, this flocculation threshold is a minimum attraction necessary for flocculation at any concentration and the results are most applicable to dilute suspensions.

Table 3 gives CFDs for various r_c, ϕ^b, and P_c^* and indicates that there is a minimum concentration of $\phi^b \approx 0.0025$ for steric stabilization for $r_c = 1000$, $P_c^* = 1000$, and 1200 atm. For a higher P_c^* of 1400 atm, the $r_c = 3000$ chains stabilize the surfaces at a lower concentration of 0.001, because the greater adsorption of the less soluble and longer polymer produces thicker layers. Stabilization may be achieved at lower concentrations by adjusting the CED to achieve an optimum balance between affinity for the surface and good solubility (for tail extension). The CFD for the $r_c = 3000$, $P_c^* = 1400$ chain (0.865) occurs somewhat above the UCSD (0.825), due to the influence of Hamaker attractive forces. A slightly higher concentration of 0.0025 produces a thicker layer that screens the Hamaker attraction at lower densities, thus shifting the CFD closer to the UCSD.

A complete understanding of the contributions to the repulsive and attractive terms in ΔG_{scf} requires consideration of the entropy and enthalpy changes. To determine the entropy change, we performed LFSCF calculations in 0.1 degree intervals from 335.7 to 336.3 K. The entropy was determined numerically from $\Delta S = -(\partial \Delta G/\partial T)_P$ and the enthalpy change was found by $\Delta H = \Delta G + T\Delta S$ (Figure 7). Figure 7a gives ΔG_{scf} for $\phi^b = 10^{-3}$. In Figure 7b, the enthalpy change is positive upon initial approach of the surfaces ($M > 2h$) because solvent is pushed from between the surfaces into the

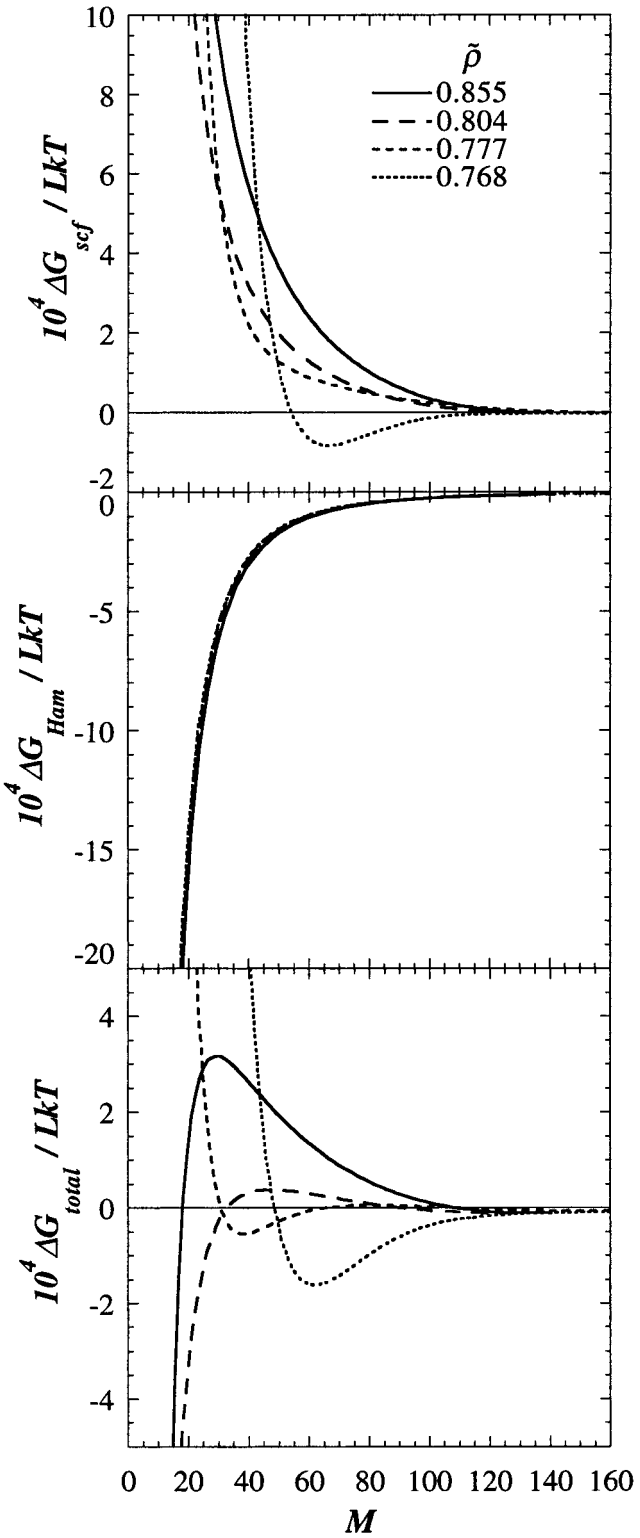

Figure 6. Interaction free energies versus separation distance, M, for two homopolymer-coated surfaces at a series of bulk solution densities. (a) $\Delta G_{scf}/LkT$; (b) $\Delta G_{Ham}/LkT$; and (c) $\Delta G_{total}/LkT$. The restricted equilibrium convention is used as described in text. The adsorbed amounts at each bulk solution density correspond to those in Figure 4: $r_c = 1000$, $\phi^b = 2.5 \times 10^{-3}$, $P_c^* = 1200$ atm, and $\epsilon_{AW} = 0.5\ kT$.

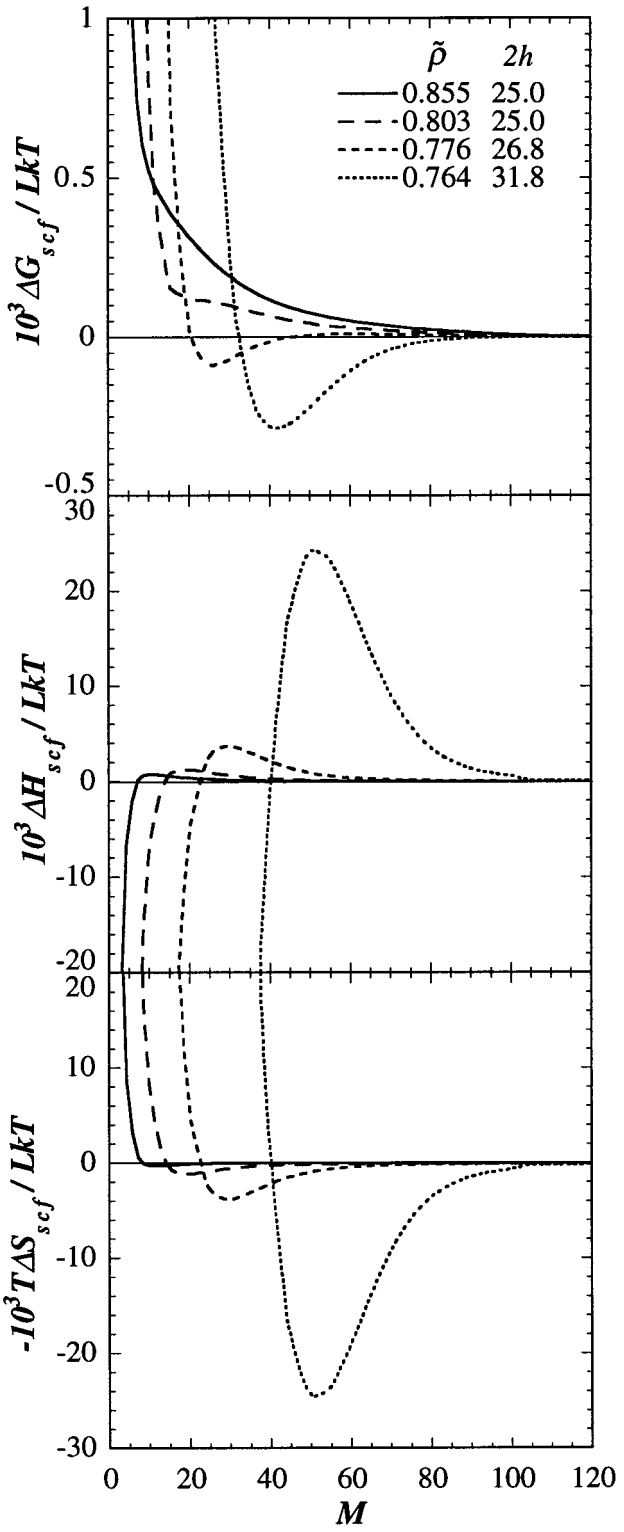

Figure 7. Interaction free energy (a), enthalpy (b), and entropy (c) versus separation distance, M, for two homopolymer-coated surfaces at a series of bulk solution densities: $r_c = 1000$, $\phi^b = 10^{-3}$, $P_c^* = 1200$ atm, and $\epsilon_{AW} = 0.5\ kT$.

lower density bulk region, sacrificing the energetic interactions with polymer in the higher density surface region (i.e., $\Delta E > 0$). The corresponding increase in system volume (not shown) also contributes to the positive enthalpy change (i.e., $\Delta H = \Delta E + P\Delta V$). In competition with this enthalpic repulsion is an *entropic attraction* (Figure 7c) that is due to the entropy gained by solvent when it expands from the high-density

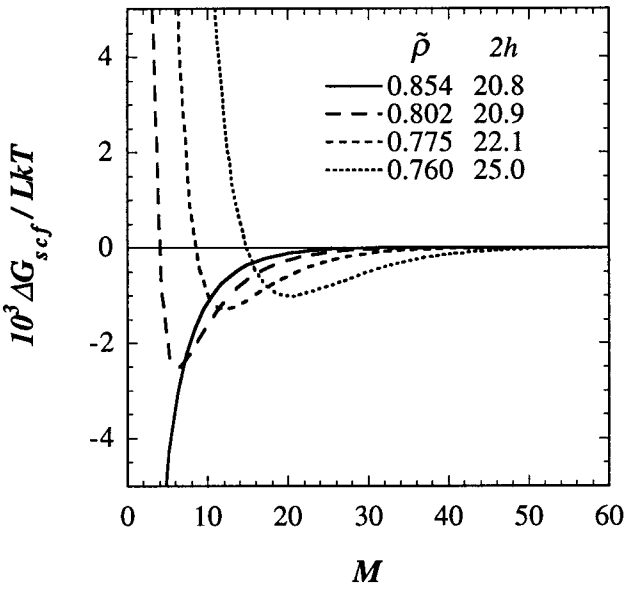

Figure 8. Interaction free energy, $\Delta G_{scf}/LkT$, versus separation distance, M, for two homopolymer-coated surfaces at a series of bulk densities: $r_c = 1000$, $\phi^b = 10^{-4}$, $P_c^* = 1200$ atm, $\epsilon_{AW} = 0.5\ kT$.

interfacial region to the lower-density bulk region.[18] Enthalpic repulsion overwhelms entropic attraction at densities above the UCSD, stabilizing the surfaces. Below the UCSD, entropic attraction overwhelms the positive enthalpy change and the surfaces are attractive. This behavior is analogous to the LCST-type phase separation of polymer−solvent mixtures in bulk.

As the surfaces are compressed to $M < 2h$ (values of $2h$ are given in Figure 7a), considerable overlap of the polymer tails occurs, resulting in lost entropy and repulsion (Figure 7c). The enthalpy simultaneously becomes negative because of favorable chain−chain intermolecular interactions. Because the chain and solvent P_i^* are different, chain−chain and solvent−solvent interactions are preferred over chain−solvent mixing. At these close distances, entropic repulsion overwhelms the enthalpic attraction and the surfaces are repulsive at all densities.

Figure 8 shows the free energy of interaction at a lower concentration of $\phi^b = 10^{-4}$. In contrast to the $\phi^b \geq 2.5 \times 10^{-3}$ cases, at the highest densities, the surfaces are not repulsive but attractive, because of bridging and entropic (LCST-type) attraction. The minima in the profiles at $\tilde{\rho} >$ UCSD occur at separations closer than the equilibrium tail thickness and a tail may attach to both surfaces simultaneously. Bridging occurs at high densities because the surface coverage is low (only 6−10% of the available area), leading to very negative enthalpies of interaction (not shown) between the surfaces. Therefore, enthalpic stabilization is not possible, in contrast with Figures 6 and 7. As $\tilde{\rho}$ is decreased, the attractive minimum in the free energy profile becomes *less* negative and moves to higher M values, due to excluded volume of the increasing number of adsorbed chains. As $\tilde{\rho}$ decreases, the increase in adsorption described previously creates a barrier to bridging. At densities below the UCSD, LCST-type attraction occurs, induced by the solvent entropy. When ΔG_{Ham} is added to ΔG_{scf} (not shown), the Hamaker forces contribute additional attraction at all densities because the adsorbed layer is not very thick. Therefore, colloid stability is not imparted by the adsorbed ho-

Table 4. Comparison Between Experimental and Predicted Critical Flocculation Density at $T/T_c = 1.05$[a]

source	system	onset of phase separation or flocculation (ρ/ρ_c)
experiment: phase behavior[19,20]	PFOA in compressed CO_2	1.7[a]
experiment: turbidimetry[19,20]	emulsion in CO_2 stabilized with PFOA	1.7
LFSCF theory[b]	homopolymer in bulk solution	1.6
LFSCF theory	surfaces with adsorbed homopolymer	1.6

[a] The Θ density for infinite molecular weight is virtually indistinguishable from the critical density for the 10^6 molecular weight polymer used in the experiments. [b] For LFSCF theory, $P_c^* = 1200$ atm, $r_c = 1000$, and $\phi^b = 0.0025$.

mopolymer at $\phi^b = 10^{-4}$ because an attractive well is present at all densities considered. The results in Table 3 indicate that bridging and LCST attraction cause flocculation for concentrations below $\phi^b = 10^{-3}$, for $r_c = 300-3000$ and various P_c^* values.

The decrease of bridging with an increase in adsorbed amount has been demonstrated in experiments with the surface forces apparatus in liquid solvents.[46,47] The experimentally determined free energy profiles are similar to those in Figure 8, where the minima become more positive and move to higher separation distance as adsorption increases. (See for example Figure 8 of ref 46 and Figure 6 of ref 48.) Using incompressible SCF theory, Scheutjens and Fleer[24] found that the interaction profiles of homopolymer-coated surfaces become less attractive as solvent quality decreases, in a manner similar to that shown in Figure 8. They also attribute this result to diminished bridging as adsorbed amount increases.

Comparison to Stability Experiments. The CFD was determined with turbidimetry for PEHA emulsions stabilized with homopolymer PFOA ($M_w = 1 \times 10^5$ and 1.2×10^6) in supercritical CO_2.[19] The temperature in the experiments was 45 °C, or $T/T_c = 1.05$, just as in the LFSCF calculations. In the experiments, the CFD was observed as a sharp decline in emulsion stability at the UCSD for the bulk PFOA−CO_2 solution. At concentrations of $\phi^b \geq 0.0025$, the LFSCF theory also predicts that the CFD occurs at the UCSD for $r_c = 1000$. Table 4 shows that the UCSD of 0.778 of the model corresponds to $\tilde{\rho}_\theta/\tilde{\rho}_c = 1.6$, which is very close to the experimental reduced CFD of 1.7.

The LFSCF results can also be compared with latexes produced by precipitation in a compressed fluid antisolvent.[11] Here, microparticles were formed by spraying a polymer solution through a nozzle into an antisolvent, in this case CO_2, at 23 °C and 124.1 bar, above the UCSD for the PFOA stabilizer. Without stabilizer, large agglomerated particles >50 μm in size were formed. Addition of 0.01 to 0.05 wt % ($\phi^b \approx 10^{-4}$ and 5×10^{-4}) PFOA ($M_w = 1 \times 10^6$) adds significant stability to the PMMA latex, resulting in slightly flocculated particles 1−4 μm in size. A further increase in PFOA concentration to 1 wt % ($\phi^b \approx 10^{-2}$) removes flocculation almost completely, yielding a particle size of <0.1 μm.

At concentrations below $\phi^b = 10^{-3}$, LFSCF theory predicts that bridging makes any correlation between bulk and surface phase behavior impossible (Table 3). Because of bridging, the correlation between flocculation and the UCSD for homopolymer stabilizers in bulk solution is a sensitive function of concentration and adsorbed amount, more so than for block copolymer or grafted stabilizers.[29] Indeed, bridging occurred in stability experiments with PFOA ($M_w = 1.2 \times 10^6$), as indicated by irreversible flocculation.[19] However, turbidimetry[19] and dynamic light scattering experiments in CO_2[20] with homopolymer PFOA indicate that the correspondence between the CFD and UCSD does not depend on stabilizer concentration between $\phi^b \approx 0.0005$ and 0.005. This result appears to contradict the LFSCF results where distinct changes in stability are observed as a function of concentration. The most likely reason for this difference is that the chain lengths used in the experiments are 2 to 10 times longer than those in the LFSCF calculations, which results in higher adsorbed amounts and a more effective barrier to bridging in the experiments. In addition, some caution is needed in comparing the experiments to the LFSCF theory because of the possible presence of nonequilibrium effects in the experiments. Adsorption and rearrangements in adsorbed chains that are at equilibrium in the LFSCF calculations may not reach equilibrium in a real system in the time scale of a collision. If the required time to form a bridge in the experimental system exceeds the collision time, then the amount of bridging will be less than that predicted by the LFSCF calculation.

Conclusions

The LFSCF calculations provide insight into the rich solvent density-dependent behavior of homopolymer adsorption in supercritical or compressible solvents. As solvent density and thus solvent quality are reduced, the tails of adsorbed polymer chains collapse. At the same time the adsorbed amount increases, especially near the UCSD of the homopolymer in bulk solution, which expands the adsorbed layer due to the excluded volume of the chains. Competition between the loss in solvent quality and the increase in excluded volume causes a collapse-to-expansion transition, indicated by a minimum in the thickness just above the UCSD.

Free energies of interaction indicate that above a threshold polymer concentration, bridging is absent, and at high densities, colloidal particles are stabilized enthalpically (for separation distances >2 h) and entropically (for separation distances < 2h). The enthalpic repulsion decreases with decreasing bulk density. Just below the UCSD, the entropically favorable expansion of solvent from the interface causes attraction and flocculation. The CFD is predicted to occur very close to the UCSD. Turbidimetry and light scattering experiments in supercritical fluids support this conclusion for stabilization with homopolymers.[19,20]

At lower concentrations ($\phi^b \leq 10^{-3}$), another mechanism of flocculation occurs. Due to low adsorbed amounts and surface coverages, bridging produces flocculation, even at high densities (good solvent). The bridging is diminished as solvent density is lowered and adsorbed amount is increased, and LCST (solvent entropy driven) attraction becomes dominant below the UCSD. At low concentration, the density dependence of colloidal stability is opposite that at higher concentration because the surfaces are less attractive as solvent quality decreases.

Acknowledgment. We thank Isaac Sanchez, Mark O'Neill, Matt Yates, and Simon Mawson for helpful comments. We acknowledge support from NSF (CTS-9626828), DOE (DE-FGO3-96ER14664), and the Sepa-

rations Research Program of the University of Texas. J.C.M. thanks the Eastman Chemical Company for providing a graduate research fellowship.

Appendix

The reader is referred to ref 18 for a derivation of the LFSCF equations. Here we modify the model to treat adsorbed rather than grafted chains. To perform the LFSCF calculation, a specific form of the interaction energy must be introduced. For a compressible lattice fluid, the energy of mixing is usually represented as[15]

$$U - U^* = \sum_z \tilde{\rho}(z) V^*(z) \left[\frac{1}{2} kT \sum_A \sum_B \phi_A(z) \langle \phi_B(z) \rangle \chi_{AB} \right] \quad \text{(A1)}$$

where $\phi_A(z)$ is the hard core volume fraction, and $\langle \phi_B(z) \rangle$ is the average fraction of B segments with which a segment of A in layer z can interact.[18] The parameter $V^*(z)$ is the hard core layer volume, $V(z) = n_o(z) + V^*(z)$ is the actual volume including holes, and $\tilde{\rho}(z) = V^*(z)/V(z)$ is the reduced density. The incompressible limit is represented by the absence of holes on the lattice when $\tilde{\rho}(z) = 1$. The parameter U^* is the reference energy given by

$$-\sum_z \sum_A V_A^* \phi_A P_A^*$$

which is the energy of pure components in the close packed state. The parameter P_A^* is the cohesive energy density of pure component A in the random close-packed reference fluid, and $\chi_{AB} = (P_A^{*1/2} - P_B^{*1/2})^2/kT$ under the geometric mean approximation. The P_i^* values control intra- and intersegmental interactions and are discussed in the theory section.

In a layer adjacent to a surface, chain segments feel an attractive potential with the surface, characterized by the dimensionless adsorption parameter χ_{AW}, which is not to be confused with the Flory interaction parameters. The parameter χ_{AW} is given by $-\epsilon_{AW}/(v^*\lambda_1)$, where ϵ_{AW} is the energy of adsorption of an anchor segment relative to that of a solvent segment and is identical to χ_s used by Scheutjens and Fleer. The parameter ϵ_{AW} is given in units of kT and is positive when A segments are attracted to the surface. The λ_1 factor represents the coordination number of surface segments that can interact with a chain segment in the first layer ($\lambda_1 = 1/4$ for a hexagonal lattice).

In the LFSCF calculations, the initial input includes the bulk chain volume fraction, the temperature, and the pressure. Pressure is chosen to yield the desired bulk density. A solution algorithm consists of specifying initial guesses for the segment potentials, $\{u_A(z)\}$, defined in ref 18, and iterating over the LFSCF equations until a consistent set of chain, solvent, and hole concentrations is found in each layer. In the bulk (far from the surface), the LFSCF model reduces properly to the lattice-fluid equation of state.[16] This equation of state is used to calculate the bulk density and chemical potentials needed to solve the LFSCF equations.

References and Notes

(1) Bartscherer, K. A.; Renon, H.; Minier, M. *Fluid Phase Equilib.* **1995**, *107*, 93−150.
(2) McFann, G. J.; Johnston, K. P. In *Microemulsions: Fundamental and Applied Aspects*; Kumar, P., Ed., in press.
(3) Yazdi, A. V.; Lepilleur, C.; Singley, E. J.; W., L.; Adamsky, F. A.; Enick, R. M.; Beckman, E. J. *Fluid Phase Equilib.* **1996**, *117*, 297−303.
(4) Shaffer, K. A.; Jones, T. A.; Canelas, D. A.; DeSimone, J. M.; Wilkinson, S. P. *Macromolecules* **1996**, *29*, 2704−2706.
(5) Canelas, D. A.; Betts, D. E.; DeSimone, J. M. *Macromolecules* **1996**, *29*, 2818−2821.
(6) DeSimone, J. M.; Maury, E. E.; Menceloglu, Y. Z.; McClain, J. B.; Romack, T. J.; Combes, J. R. *Science* **1994**, *265*, 356−359.
(7) Adamsky, F. A.; Beckman, E. J. *Macromolecules* **1994**, *27*, 312−314.
(8) DeSimone, J. M.; Guan, Z.; Elsbernd, C. S. *Science* **1992**, *257*, 945−947.
(9) Hsiao, Y.-L.; Maury, E. E.; M., D. J.; Mawson, S.; Johnston, K. P. *Macromolecules* **1995**, *28*, 8159.
(10) Mawson, S.; Johnston, K. P.; Combes, J. R.; DeSimone, J. M. *Macromolecules* **1995**, *28*, 3182−3191.
(11) Mawson, S.; Yates, M. Z.; O'Neill, M. L.; Johnston, K. P. *Langmuir* **1997**, *13*, 1519−1528.
(12) Hoefling, T. A.; Beitle, R. R.; Enick, R. M.; Beckman, E. J. *Fluid Phase Equilib.* **1993**, *83*, 203-212.
(13) Hoefling, T. A.; Enick, R. M.; Beckman, E. J. *J. Phys. Chem.* **1991**, *95*, 7127−7129.
(14) Luna-Bárcenas, G.; Meredith, J. C.; Gromov, D. G.; Sanchez, I. C.; de Pablo, J. J.; Johnston, K. P. *J. Chem. Phys.* **1997**, *107*, 1−11.
(15) Sanchez, I. C. In *Encyclopedia of Physical Science and Technology*; Academic: New York, 1987; Vol. XI, pp 1−18.
(16) Sanchez, I. C.; Panayiotou, C. G. In *Models for Thermodynamic and Phase Equilibria Calculations*; Sandler, S., Ed.; Dekker: New York, 1993; Vol. 52, pp 187−285.
(17) Napper, D. H. *Polymeric Stabilization of Colloidal Dispersions*; Academic: London, 1983.
(18) Peck, D. G.; Johnston, K. P. *Macromolecules* **1993**, *26*, 1537−1545.
(19) O'Neill, M. L.; Yates, M. Z.; Johnston, K. P.; Wilkinson, S. P.; Canelas, D. A.; Betts, D. E.; DeSimone, J. M. *Macromolecules* **1997**, *30*, 5050−5059.
(20) Yates, M. Z.; O'Neill, M. L.; Johnston, K. P.; Webber, S.; Canales, D. A.; Betts, D. A.; DeSimone, J. M. *Macromolecules* **1997**, *30*, 5060−5067.
(21) O'Neill, M. L.; Cao, Q.; Fang, M.; Johnston, K. P.; Wilkinson, S. P.; Smith, C. D.; Kerschner, J. L.; Jureller, S. H. *Ind. Eng. Chem. Res.*, in press.
(22) Mawson, S.; Johnston, K. P.; DeSimone, J. M.; Betts, D. E.; McClain, J. B. *Macromolecules* **1997**, *30*, 71.
(23) Scheutjens, J. M. H. M.; Fleer, G. J. *J. Phys. Chem.* **1979**, *83*, 1619.
(24) Scheutjens, J. M. H. M.; Fleer, G. J. *Macromolecules* **1985**, *18*, 1882−1900.
(25) Evers, O. A.; Scheutjens, J. M. H. M.; Fleer, G. J. *Macromolecules* **1990**, *23*, 5221−5233.
(26) Evers, O. A.; Scheutjens, J. M. H. M.; Fleer, G. J. *Macromolecules* **1991**, *24*, 5558−5566.
(27) Zhulina, E. B.; Borisov, O. V.; Pryamitsyn, V. A.; Birshtein, T. M. *Macromolecules* **1991**, *24*, 140−149.
(28) Szleifer, I.; Carignano, M. A. *Adv. Chem. Phys.* **1996**, *94*, 165−260.
(29) Meredith, J. C.; Johnston, K. P. *Macromolecules* **1998**, *31*, 5518−5528.
(30) Fleer, G. J.; Cohen Stuart, M. A.; Schuetjens, J. M. H. M.; Cosgrove, T.; Vincent, B. In *Polymers at Interfaces*; Chapman and Hall: London, 1993; p 282.
(31) Wang, Y.; Mattice, W. L. *Langmuir* **1994**, *10*, 2281−2288.
(32) Cosgrove, T.; Heath, T.; van Lent, B.; Leermakers, F.; Scheutjens, J. *Macromolecules* **1987**, *20*, 1692−1696.
(33) Hunter, R. J. *Australian J. Chem.* **1963**, *16*, 774−778.
(34) Sanchez, I. C.; Lacombe, R. H. *J. Phys. Chem.* **1976**, *80*, 2352−2362.
(35) van der Beek, G. P.; Cohen Stuart, M. A.; Fleer, G. J. *Langmuir* **1989**, *5*, 1180−1186.
(36) Scheutjens, J. M. H. M.; Fleer, G. J. C. S., M. A. *Colloids Surf.* **1986**, *21*, 285−306.
(37) Lyklema, J. *Fundamentals of Interface and Colloid Science. Volume I: Fundamentals*; Academic: London, 1991.
(38) Prausnitz, J., M.; Lichtenthaler, R., N.; de Azevedo, E. G. *Molecular Thermodynamics of Fluid Phase Equilibria*; Prentice Hall: Englewood Cliffs, NJ, 1986.
(39) Kawaguchi, M.; Takahashi, A. *J. Polym. Sci., Polym. Phys. Ed.* **1980**, *18*, 2069−2076.
(40) Kawaguchi, M.; Takahashi, A. *Macromolecules* **1983**, *16*, 1469−1475.

(41) Kawaguchi, M.; Yamagiwa, S.; Takahashi, A.; Kato, T. *J. Chem. Soc., Faraday Trans.* **1990**, *86*, 1383−1387.
(42) Takahashi, A.; Kawaguchi, M. *Adv. Polym. Sci.* **1982**, *46*, 47−50.
(43) Flory, P. J. *Principles of Polymer Chemistry*; Cornell University: New York, 1953.
(44) Hu, H.-W.; Granick, S. *Macromolecules* **1990**, *23*, 613−623.
(45) Gao, J.; Wu, C. *Macromolecules* **1997**, *30*, 6873−6876.
(46) Almog, Y. a.; Klein, J. *J. Colloid Interface Sci.* **1985**, *106*, 33−44.
(47) Israelachvili, J. N.; Tirrell, M.; Klein, J.; Almog, Y. *Macromolecules* **1984**, *17*, 204−209.
(48) Ruths, M.; Israellachvili, J. N.; Ploehn, H. J. *Macromolecules* **1997**, *30*, 3329−3339.

MA980259Q